

## Color-Tunable Photoluminescence of Alloyed $\text{CdS}_x\text{Se}_{1-x}$ Nanobelts

Anlian Pan,<sup>†,‡</sup> Hua Yang,<sup>‡</sup> Ruibin Liu,<sup>†,‡</sup> Richeng Yu,<sup>‡</sup> Bingsuo Zou,<sup>\*,†,‡</sup> and Zhonglin Wang<sup>\*,§</sup>

*Micro-Nano Technologies Research Center, Hunan University, Changsha 41008, China, Institute of Physics, Chinese Academy of Sciences, Beijing 100080, China, and School of Materials Science and Engineering, Georgia Institute of Technology, Atlanta, Georgia 30332-0245*

Received September 6, 2005; E-mail: zoubs@aphy.iphy.ac.cn

Wide band gap semiconductor nanowires and nanobelts, such as ZnO, CdS, as the 1D nanostructure, recently have received considerable attention for their special properties and applications in sensors, lasers, waveguides, and optoelectronic devices.<sup>1–6</sup> For devices in nanoelectronics and nanophotonics, it is very important to fabricate materials with continuous tunable physical properties. Recent advances in ternary semiconductor nanocrystals or films have shown that their band gaps and then their optical emissions can be tuned by changing their constituent stoichiometries,<sup>7–12</sup> while such study is few for the ternary semiconductors with 1D nanostructures.

Very recently, Lee's group reported the fabrication of  $\text{Zn}_x\text{Cd}_{1-x}\text{S}$  nanoribbons by a laser ablation-assisted CVD route and realized the tunable PL emission in the region from ultraviolet ( $\sim 340$  nm) to green light ( $\sim 515$  nm).<sup>13</sup> In this paper, we report for the first time the synthesis of single crystal ternary  $\text{CdS}_x\text{Se}_{1-x}$  nanobelts with site-controlled compositions via a simple one-step physical evaporation process and the observation of their color-tunable PL emissions from green ( $\sim 508$  nm) to the near-infrared ( $\sim 705$  nm).

The  $\text{CdS}_x\text{Se}_{1-x}$  ( $0 \leq x \leq 1$ ) nanobelts were synthesized based on the physical evaporation of commercial-grade CdS and CdSe (Alfa Aesar, 99.995% purity) in the presence of a Au catalyst following that demonstrated for CdSe nanobelts and nanosaws.<sup>14</sup> To prepare the ternary  $\text{CdS}_x\text{Se}_{1-x}$ , a 1 g mixture of CdS and CdSe powders (mole ratio 1:1) was placed onto a ceramic plate at the center of a quartz tube, which was inserted into a horizontal tube furnace. Several pieces of silicon slices coated with  $\sim 2$  nm Au film were placed downstream of the gas flow and separately about 8–14 cm from the center of the ceramic plate. Prior to heating, high-purity He was introduced into the quartz tube with a constant flowing rate (20 sccm) to purge the  $\text{O}_2$  inside. After 100 min, the furnace was rapidly heated to 900 °C and maintained at 900 °C for 60 min. Bright yellow to brown–red products were deposited on the surface of the silicon wafer at the deposition temperature of 650–800 °C downstream. CdS or CdSe nanobelts were prepared through the same procedure, except using only CdS or CdSe powder as the evaporation source.

The morphologies of the as-prepared samples at different substrate temperatures show little variation and are all sword-like nanobelts (Figure 1a), with the typical length of 20–60  $\mu\text{m}$  and a thickness of 40–80 nm. The width is 100 nm to 1  $\mu\text{m}$  at one end and tapers off to a  $\sim 50$ –100 nm tip at the other end. The elemental compositions of these nanobelts were investigated using in situ energy-dispersive X-ray spectroscopy (EDS), which shows that all of the samples, except the pure CdS and CdSe, contain Cd, S, and Se, and the atomic ratios of (S+Se)/Cd are all very close to 1, but the relative ratios of S to Se are highly dependent on the distance

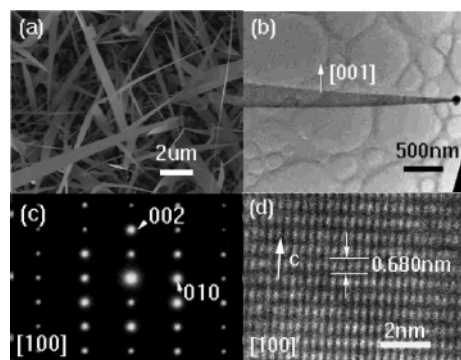


**Figure 1.** (a) Typical SEM morphology of the obtained ternary  $\text{CdS}_x\text{Se}_{1-x}$  nanobelts. (b) TEM image of a single ternary nanobelt; (c and d) its selected area electron diffraction (SAED) pattern and HRTEM image, respectively.

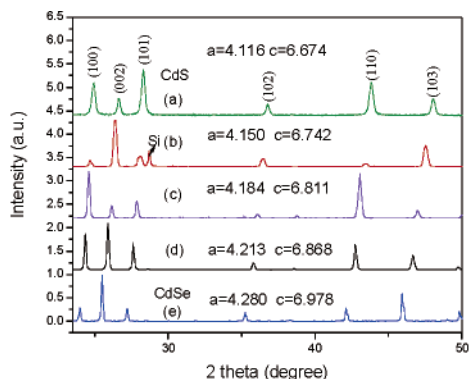
of the silicon wafer from the location of source materials (see the Supporting Information Figure S1). That is, the mole fraction of S (or Se) monotonically increases (or decreases) from high to low substrate temperature. Moreover, the distributions of elements S and Se in the nanobelts are very homogeneous, which can be confirmed by element mapping (see the Supporting Information Figure S2). The composition change with deposition temperature is similar to that of the  $\text{Zn}_x\text{Cd}_{1-x}\text{S}$  nanobelts fabricated by the laser ablation-assisted CVD route.<sup>13</sup> Figure 1b shows a TEM image of a representative single ternary nanobelt with a catalytic particle at the sharp tip. The selected area electron diffraction pattern (Figure 1c) confirms the single-crystal quality of the belt and can be indexed to have a hexagonal structure with lattice parameters of  $a = 0.418$  nm and  $c = 0.678$  nm. The corresponding HRTEM image (Figure 1d) further demonstrates a single-crystalline structure with 0.680 nm lattice spacing, corresponding to the (001) interplanar distance of hexagonal  $\text{CdS}_x\text{Se}_{1-x}$ . The formation of the alloyed nanobelts is likely to follow the VLS+VS growth mechanism, proposed for the growth of the CdSe nanobelts.<sup>15</sup>

Figure 2 shows the normalized X-ray diffraction patterns of several representative  $\text{CdS}_x\text{Se}_{1-x}$  ( $0 \leq x \leq 1$ ) samples. Curves (a) and (e) are for the CdS and CdSe nanobelts, respectively, which are consistent with respective bulk wurtzite CdS (JCPDS 41-1049) and CdSe (JCPDS 77-2309) crystals. Curves (b)–(d) are the samples in queue deposited on the substrate with gradually rising temperature. It is clearly seen that the crystallographic phase of all the samples is in good agreement with that of the typical hexagonal wurtzite crystals. The diffraction peaks from curve (a) to (e) shift gradually toward low angles, indicating that the lattice constants of the belts increase with the S concentration decreases. The fitted lattice cell parameters for these samples are labeled above the corresponding curves in Figure 2. According to Vegard's law for ternary  $\text{CdS}_x\text{Se}_{1-x}$  compounds,<sup>11</sup> the lattice parameters have a linear dependence on the composition  $x$ , according to  $c(x) = x \times c_{\text{CdS}} + (1 - x) \times c_{\text{CdSe}}$ , where  $c_{\text{CdS}}$ ,  $c_{\text{CdSe}}$ , and  $c(x)$  are the respective  $c$ -axis

<sup>†</sup> Hunan University.

<sup>‡</sup> Chinese Academy of Sciences.

<sup>§</sup> Georgia Institute of Technology.



**Figure 2.** The normalized X-ray diffraction patterns of several  $\text{CdS}_x\text{Se}_{1-x}$  ( $0 \leq x \leq 1$ ) samples. Curves (a) and (e) are for the CdS and CdSe nanobelts, respectively. Curves (b)–(d) are, in turn, for the samples at the deposition position with gradually increasing temperature. The peak at  $28.7^\circ\text{C}$  of curve (b) is from the Si substrate.

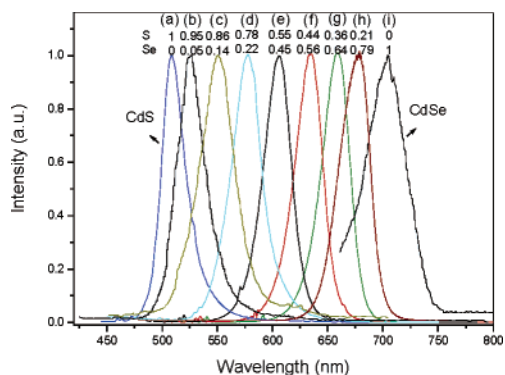


**Figure 3.** The normalized PL spectra of the obtained  $\text{CdS}_x\text{Se}_{1-x}$  nanobelts excited with a He–Cd laser (325 nm). Curves (a) and (i) are the PL spectra for CdS and CdSe nanobelts, respectively, and curves (b)–(h) are for the  $\text{CdS}_x\text{Se}_{1-x}$  nanobelts collected at  $\sim 650$ , 670, 695, 720, 745, 770, and  $800^\circ\text{C}$ , respectively. The data above the spectra show the relative concentrations of S and Se in the corresponding sample.

lattice constants of the hexagonal structured CdS, CdSe, and  $\text{CdS}_x\text{Se}_{1-x}$ . The composition  $x$  of the nanobelts can be determined from Vegard's law using the lattice parameters deduced from the XRD data. For samples shown in Figure 2b–d, the determined compositions are, respectively,  $\text{CdS}_{0.78}\text{Se}_{0.22}$ ,  $\text{CdS}_{0.55}\text{Se}_{0.45}$ , and  $\text{CdS}_{0.36}\text{Se}_{0.64}$ , in good agreement with the results from EDS (see the Supporting Information Figure S3). The above results indicate that alloyed  $\text{CdS}_x\text{Se}_{1-x}$  nanobelts with modulated compositions between CdS and CdSe were successfully obtained at the different temperature region during this simple physical evaporation process.

Figure 3 shows the normalized photoluminescence (PL) spectra of the obtained  $\text{CdS}_x\text{Se}_{1-x}$  nanobelts excited with a He–Cd laser (325 nm). Curves (a) and (i) are the PL spectra for CdS and CdSe nanobelts, respectively, and curves (b)–(h) are for the  $\text{CdS}_x\text{Se}_{1-x}$  nanobelts collected at  $\sim 650$ , 670, 695, 720, 745, 770, and  $800^\circ\text{C}$ , respectively. The spectra of all-site samples show a single emission band related to near-bandedge recombination, and the spectral peaks for these ternary nanobelts continuously shift toward low energy with increasing the local deposition temperature, in the spectral range from  $\sim 508$  nm (for pure CdS) to  $\sim 705$  nm (for pure CdSe). As reported in refs 11 and 12, the band gap of ternary  $\text{CdS}_x\text{Se}_{1-x}$  films becomes larger with increasing the composition  $x$ ,<sup>11,12</sup> and

the PL spectrum maxima of our samples are in good agreement with the results of the corresponding  $\text{CdS}_x\text{Se}_{1-x}$  films,<sup>11</sup> so the spectral shift of the bandedge emission of the alloyed nanobelts with the deposition temperature should come from the variety of their band gap energy, due to the different relative composition of Se or S. At the same time, the continuous shift of the PL bands for the obtained nanobelts with their compositions gives further evidences for the formation of the alloyed  $\text{CdS}_x\text{Se}_{1-x}$  nanobelts via intermixing the wide band gap of CdS (2.48 eV) and the narrow band gap of CdSe (1.77 eV), rather than the formation of the independent CdS and CdSe nanobelts. In contrast, the PL spectra of all the nanobelts only have the bandedge emission, but the  $\text{CdS}_x\text{Se}_{1-x}$  films or microcrystals<sup>11,12</sup> simultaneously show a defect or structural disorder-related low-energy emission in their PL spectrum besides the bandedge emission. The absence of low-energy emission band of our samples further demonstrates that the obtained nanobelts are highly crystallized with few defects. Furthermore, it is worth noting that the bandedge emission of these ternary  $\text{CdS}_x\text{Se}_{1-x}$  nanobelts is very strong at room temperature, indicating their potential applications in adjustable nano/micro optoelectronic devices in the visible region.

In summary, we have successfully synthesized single-crystal  $\text{CdS}_x\text{Se}_{1-x}$  nanobelts of variable composition ( $0 \leq x \leq 1$ ) by a very simple one-step evaporation route. PL measurements showed that all the  $\text{CdS}_x\text{Se}_{1-x}$  nanobelts have a strong single emission band near their bandedges, and these spectral peaks could shift from  $\sim 508$  nm (for pure CdS) to  $\sim 705$  nm (for pure CdSe). This work shows the feasibility to tune PL emissions, covering the whole visible spectral range, of 1D ternary semiconductor nanostructures. This finding may find significant applications in the tunable nano/micro photoelectric devices in the visible region.

**Acknowledgment.** The authors are grateful for the financial support of the Nano fund of Hunan University, National 973 Project, Nano and Bio-device Key Project of CAS.

**Supporting Information Available:** EDS spectra, element mapping, and the method for composition decision. This material is available free of charge via the Internet at <http://pubs.acs.org>.

## References

- Duan, X.; Huang, Y.; Argarwal, R.; Lieber, C. M. *Nature* **2002**, *421*, 24.
- Law, M.; Sirbuly, D. J.; Johnson, J. C.; Goldberger, J.; Savkallv, R. J.; Yang, P. *Science* **2004**, *305*, 1269.
- Sun, X. W.; Kwok, H. S. *J. Appl. Phys.* **1999**, *86*, 408.
- Pan, Z. W.; Dai, Z. R.; Wang, Z. L. *Science* **2001**, *291*, 1947.
- Huang, Y.; Duan, X.; Lieber, C. M. *Small* **2005**, *1*, 142.
- Pan, A.; Liu, D.; Liu, R.; Wang, F.; Zou, B. *Small* **2005**, *1*, 980.
- Zhong, X.; Feng, Y.; Knoll, W.; Han, M. *J. Am. Chem. Soc.* **2003**, *125*, 13559.
- Bailey, R. E.; Nie, S. *J. Am. Chem. Soc.* **2003**, *125*, 7100.
- Petrov, D. V.; Santos, B. S.; Pereira, G. A. L.; Donega, C. D. M. *J. Phys. Chem. B* **2002**, *106*, 5325.
- Kulkarni, S. K.; Winkler, U.; Deshmukh, N.; Borse, P. H.; Fink, R.; Umbach, E. *Appl. Surf. Sci.* **2001**, *169*, 438.
- Perna, G.; Pagliara, S.; Capozzi, V.; Ambrico, M.; Ligongo, T. *Thin Solid Films* **1999**, *349*, 220.
- Meit, G. *J. Phys.: Condens. Matter* **1992**, *4*, 7521.
- Liu, Y.; Zapien, J. A.; Shan, Y. Y.; Geng, C. Y.; Lee, C. S.; Lee, S. T. *Adv. Mater.* **2005**, *17*, 1372.
- Ma, C.; Ding, Y.; Moore, D.; Wang, X.; Wang, Z. *J. Am. Chem. Soc.* **2004**, *126*, 708.
- Venugopal, R.; Lin, P.; Liu, C.; Chen, T. *J. Am. Chem. Soc.* **2005**, *127*, 11262.

JA056116I